Am J Transl Res 2018;10(3):696-708
www.ajtr.org /ISSN:1943-8141/AJTR0066361

Original Article

YM155 enhances docetaxel efficacy in ovarian cancer

Li-Jiao Hou[1*], Xiao-Xiu Huang[1*], Li-Na Xu[1], Yan-Yan Zhang[1], Na Zhao[1], Rong-Ying Ou[1], Wen-Feng Li[3], Wen-Ji Zhang[2], Qi-Wei Jiang[2], Yang Yang[2], Meng-Ning Wei[2], Jia-Rong Huang[2], Kun Wang[2], Meng-Ling Yuan[2], Zi-Hao Xing[2], Zhi Shi[2], Xiao-Jian Yan[1]

[1]Department of Gynecology, The First Affiliated Hospital of Wenzhou Medical University, Wenzhou 325000, Zhejiang, China; [2]Department of Cell Biology & Institute of Biomedicine, National Engineering Research Center of Genetic Medicine, Guangdong Provincial Key Laboratory of Bioengineering Medicine, College of Life Science and Technology, Jinan University, Guangzhou 510632, Guangdong, China; [3]Department of Chemoradiotherapy, The First Affiliated Hospital of Wenzhou Medical University, Wenzhou 325000, Zhejiang, China. [*]Equal contributors.

Received September 22, 2017; Accepted December 24, 2017; Epub March 15, 2018; Published March 30, 2018

Abstract: YM155 (Sepantronium bromide) is a potent small molecule inhibitor of survivin by suppression of survivin expression and shows the promising anticancer activity in many types of cancers. Docetaxel (Taxotere®) is a member of the taxane drugs used in the treatment of a number of cancers in clinic. Despite the therapeutic efficacy of docetaxel is encouraging, the emergent resistance is an urgent issue. In this study, we investigate the effect of YM155 on docetaxel efficacy in ovarian cancer cells. Our data showed that YM155 actively induced cell growth inhibition, cell cycle arrest and apoptosis with downregualtion of survivin in ovarian cancer cells. Moreover, YM155 increased the intracellular ROS levels, and pretreatment with either NAC or GSH partially reversed the YM155-induced ROS accumulation and apoptosis only in the parental A2780 cells, but not in the resistant A2780/Taxol cells. Furthermore, YM155 enhanced docetaxel efficacy to inhibit the growth and induce apoptosis in ovarian cancer cells. Take together, our results suggested that combination of YM155 and docetaxel may be a feasible strategy for the treatment of ovarian cancer.

Keywords: Ovarian cancer, YM155, docetaxel

Introduction

Docetaxel (Taxotere®) is a member of the taxane drugs, which is a class of diterpenes derived from the genus Taxus (yews) including paclitaxel (Taxol®), baccatin III, etc. Taxanes act as mitotic inhibitors by stabilizing the microtubule polymer to protect it from disassembly, which results in chromosomes unable to form a metaphase spindle configuration, therefore suppressing mitosis progress and inducing cell death [1]. Currently, docetaxel is used in the treatment of a number of cancers including lung, breast, prostate, gastric, ovarian cancer, and so on. Despite the therapeutic efficacy of docetaxel is encouraging in clinic, the emergent resistance is becoming an important issue. Extensive work has attempted to elucidate the molecular mechanisms of docetaxel resistance, and many molecules have been implicated to involve in docetaxel resistance [1]. Overexpression or mutation of the docetaxel target, β-tubulin, is one of the common reasons of docetaxel resistance [2, 3]. Overexpressing the ATP-binding cassette (ABC) transporters such as ABCB1 (also named P-glycoprotein, P-gp), ABCC2 and ABCC10 is another cause resulting in docetaxel resistance [4, 5]. Additionally, the deficit of apoptotic cell death also contributes to docetaxel resistance, and alteration of apoptotic related genes (survivin, Bcl-2, p53, etc) are always associated with docetaxel sensitivity [6, 7]. Therefore, it is urgent to develop new therapeutic strategies to overcome docetaxel resistance or enhance docetaxel sensitivity for the treatment of cancer.

YM155 (Sepantronium bromide) is a potent small molecule inhibitor of survivin by suppression of survivin expression [8]. YM155 directly binds to the C-terminal of RNA binding proteins interleukin enhancer-binding factor-3 (ILF3/NF110) and disrupts it binding to survivin promoter, leading to downregulation of survivin

expression [9, 10]. The anticancer activity of YM155 has been demonstrated in many types of cancers, such as lung cancer, breast cancer, Hodgkin lymphoma, prostate cancer and Wilms tumor, etc [11-16]. Althouth YM155 can sensitize ovarian cancer cells to cisplatin inducing apoptosis and tumor regression [17], whether YM155 overcomes docetaxel resistance or enhances docetaxel sensitivity in ovarian cancer are still unclear. In this study, we investigate the effect of YM155 on docetaxel efficacy in ovarian cancer cells.

Material and methods

Cell culture and reagents

Human ovarian cancer cell lines A2780, A2780 /Taxol, SKOV3, OVCAR3, HO8910, HO8910PM, and ES2 were cultured in Dulbecco's modified Eagle's medium (DMEM) containing 10% fetal calf serum (FBS), penicillin (100 U/ml) and streptomycin (100 ng/ml) in a humidified incubator at 37°C. YM155 and docetaxel were ordered from ApexBio and Hengrui Medicine, respectively. N-acetly-L-cysteine (NAC), glutathione (GSH) and dihydroethidium (DHE) were purchased from Sigma-Aldrich. Anti-PARP (9542), Anti-Mcl-1 (4572), Anti-Survivin (2808), Anti-AKT (4691), Anti-pAKT S473 (4060), Anti-pERK T202/Y204 (4370) and Anti-ERK (4695) antibodies were from Cell Signaling Technologies. Anti-β-tublin (KM9003T) antibodies were from Tianjin Sungene Biotech. Anti-p21 (554-262), Anti-p27 (610241), and Anti-p53 (5541-69) antibodies were from BD Biosciences. Anti-Bax (RLT0456) antibodies were from Ruiying Biotech.

Cell viability assay

Cells were firstly seeded into a 96-well plate at a density of 5000 cells per well, and incubated with drugs in three parallel wells for 72 h. Then 3-(4,5-dimethylthiazolyl-2)-2,5-diphenyltetrazolium bromide (MTT) was added to each well at a final concentration of 0.5 mg/ml. After incubation for 4 h, formazan crystals were dissolved in 100 μl of DMSO, and absorbance at 570 nm was measured by plate reader. The concentrations required to inhibit growth by 50% (IC_{50}) were calculated from survival curves using the Bliss method [18, 19]. For drug combination experiments, cells were co-treated with different concentrations of YM155 and docetaxel for 72 h. The data were analyzed by CompuSyn software with the results showed as combination index (CI) values according to the median-effect principle, where CI <1, =1, and >1 indicate synergism, additive effect, and antagonism, respectively [20, 21].

Cell cycle assay

Cells were fixed with ice-cold 70% ethanol for 30 min at 4°C and resuspended with 0.5 ml phosphate buffered saline (PBS) containing PI (50 μg/ml), 0.1% Triton X-100, 0.1% sodium citrate, and DNase-free RNase (100 μg/ml), and 0.1% sodium citrate. After 15 min incubation at room temperature in the dark, cells was measured by flow cytometry (FCM) with an excitation wave length of 480 nm through a FL-2 filter (585 nm). Data were analyzed using ModFit LT 3.0 software (Becton Dickinson) [22, 23].

Apoptosis assay

Cells were stained with Annexin V-FITC and propidium iodide (PI) in the binding buffer, and detected by FCM after 15 min incubation at room temperature in the dark. Fluorescence was measured at an excitation wave length of 480 nm through FL-1 (530 nm) and FL-2 filters (585 nm). The apoptotic cells were quantified using FlowJO software [24, 25].

Reactive oxygen species (ROS) assay

Cells were incubated with DHE (10 μM) for 30 min at 37°C in the dark. Five fields were observed randomly for each well. ROS activation was analyzed by calculating the percentage of positive cells [26, 27].

Western blot analysis

Cells were lysed in RIPA buffer (1% NP-40, 0.5% sodium deoxycholate, 0.1% SDS, 10 ng/ml PMSF, 0.03% aprotinin, 1 μM sodium orthovanadate) at 4°C. Lysates were centrifuged for 10 min at 14,000× g. Proteins were separated on 12% SDS-PAGE gels and transferred to polyvinylidene difluoride membranes. Membranes were blocked with 5% BSA and incubated with the indicated primary antibodies. Corresponding horseradish peroxidase-conjugated secondary antibodies were used against each primary antibody. Proteins were detected using the che-

A

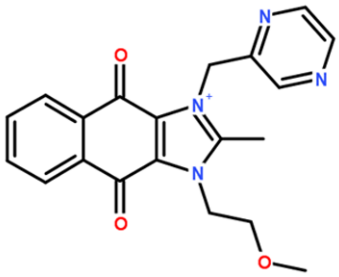

B Summary of IC50 of YM155 and Docetaxel in the ovarian cancer cells.

IC50	YM155 (nM±SD)	Docetaxel (nM±SD)
A2780	3.733±0.558	3.425±0.827
A2780/Taxol	321.3171±54.255	301.880±11.556
SKOV3	5.245±3.873	3.702±2.847
OVCAR3	5.716±0.586	2.885±0.123
HO8910	10.095±0.008	4.835±3.520
HO8910-PM	110.740±37.688	11.039±11.308
ES-2	6.491±0.00884	2.505±0.269

C

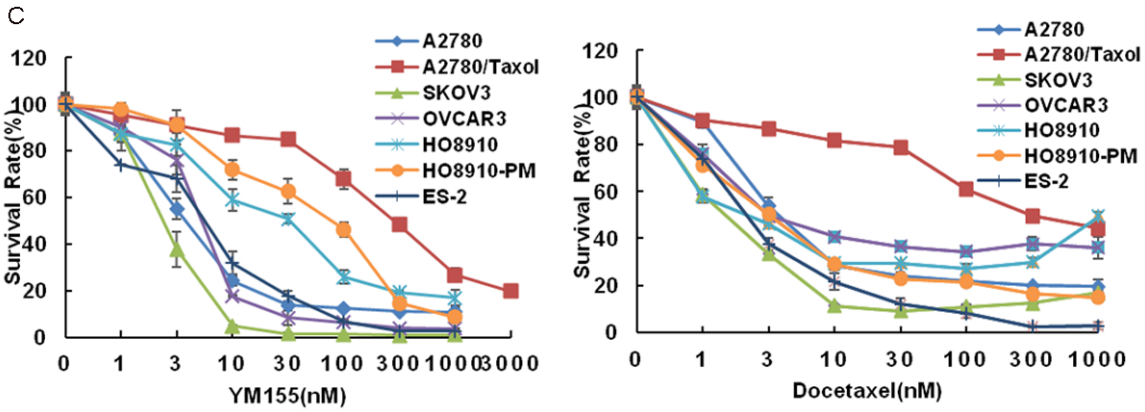

Figure 1. YM155 inhibits the growth of ovarian cancer cells. A. Chemical structure of YM155. B. Summary of IC_{50} of YM155 and docetaxel in the indicated ovarian cancer cells is shown. Cells were grown in 96-well plates for 24 h and treated with the indicated concentrations of YM155 or docetaxel for 72 h, and cell survival was determined by MTT assay. C. The representative growth curves of cells treated with YM155 and docetaxel are shown. Data are mean ± SD of three independent experiments.

miluminescent detection reagents and chemstudio plus imaging system [28, 29].

Statistical analysis

All experiments were repeated at least three times. The statistical significance between two groups was determined with Student's t-test. A probability value of $P<0.05$ was considered as significant differences.

Result

YM155 and docetaxel suppress the growth of ovarian cancer cells

To investigate the effect of YM155 on docetaxel efficacy in ovarian cancer cells, we first tested the cytotoxicity of YM155 and docetaxel in seven human ovarian cancer cells. As shown in **Figure 1**, YM155 inhibited the growth of all ovarian cancer cells in a dose-dependent manner with the IC_{50} values range from 3.73 nM to 321.31 nM. Similarly, the IC_{50} values of docetaxel in all ovarian cancer cells were range from 2.505 nM to 301.88 nM. Interestingly, the taxol resistant cells A2780/Taxol, which overexpresses ABCB1 gene [30], showed about 87 folds resistance to both YM155 and docetaxel compared with the parental A2780 cells.

YM155 induces cell cycle arrest in ovarian cancer cells

To explore whether the growth inhibition of ovarian cancer cells by YM155 is due to cell cycle arrest, cell cycle distribution was assessed after treating A2780 and A2780/Taxol cells with YM155. As shown in **Figure 2A** and **2B**, YM155 dose-dependently induced cell accumulation at S phase and reduction at G0/G1 phase in both cells. To further investigate the molecular mechanism of cell cycle arrest by YM155, the expression of cell cycle related proteins were detected by Western blot. YM155

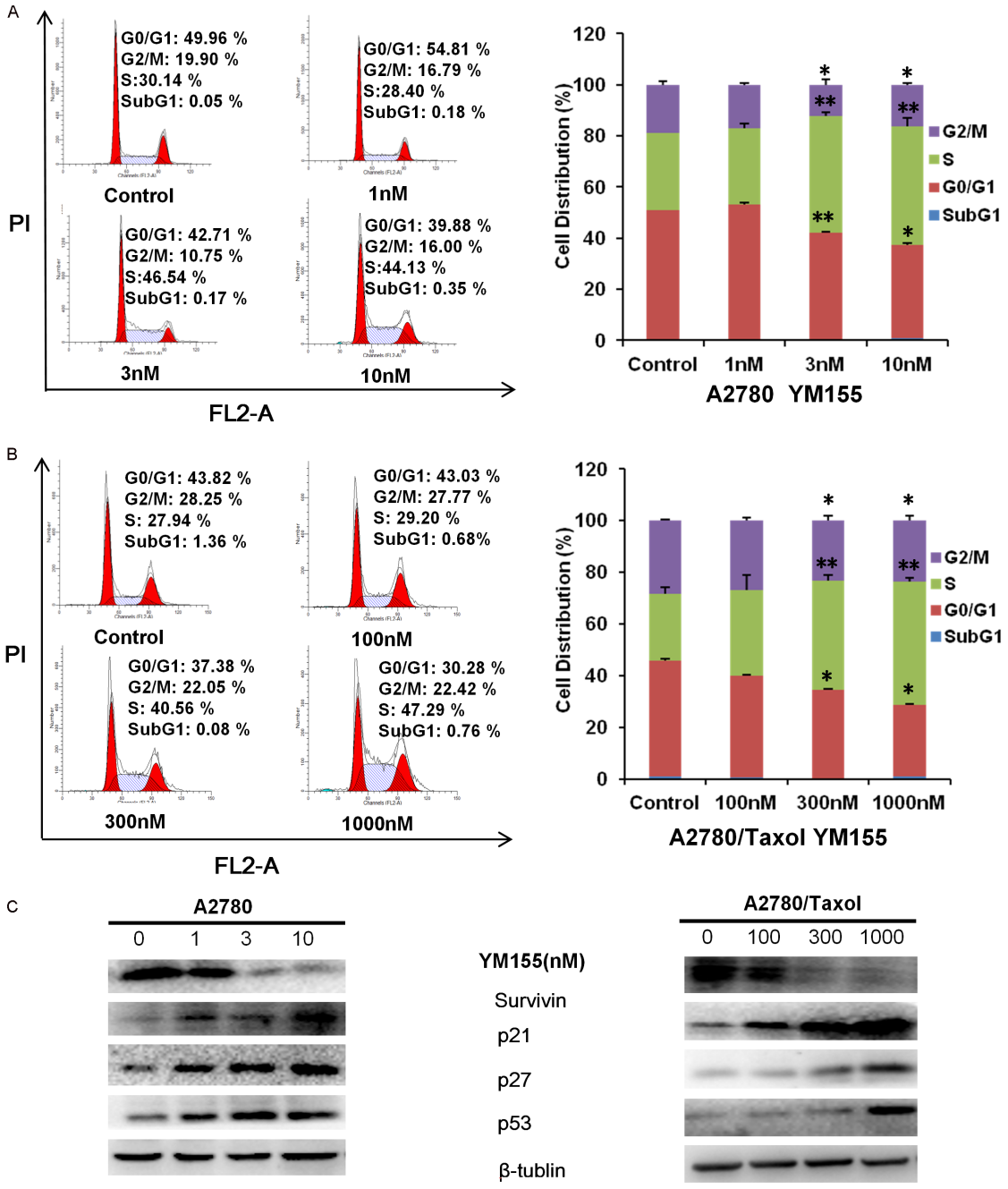

Figure 2. YM155 induces cell cycle arrest in ovarian cancer cells. A2780 (A) and A2780/Taxol (B) cells were treated with YM155 at the indicated concentrations for 48 h. The distribution of cell cycle was detected by FCM with PI staining. The percentages of subG1, G1/G0, S, G2/M phase were calculated using ModFit LT 3.0 software. The protein expression was examined by Western blot after lysing cells, and β-tublin was used as loading control. The representative charts, quantified results and Western blot results (C) of three independent experiments were shown. The statistical significance between two groups was determined with Student's t-test. **P*<0.05 and ***P*<0.01 vs. corresponding control.

dose-dependently decreased the protein levels of survivin as expected, but increased the protein levels of p21, p27 and p53 in both cells (**Figure 2C**).

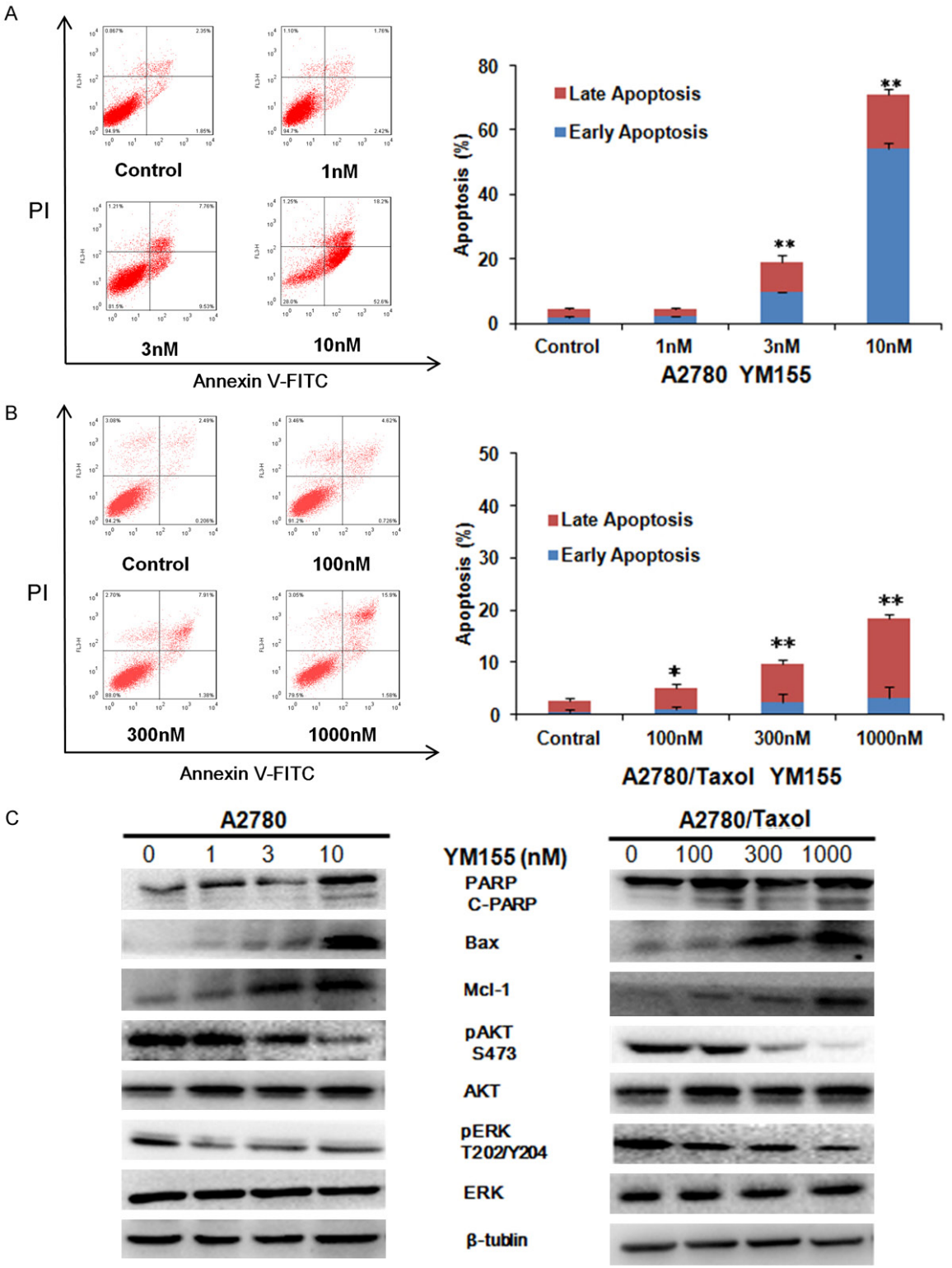

Figure 3. YM155 triggers apoptosis in ovarian cancer cells. A2780 (A) and A2780/Taxol (B) cells were treated with YM155 at the indicated concentrations for 48 h. The apoptosis was detected by FCM Annexin V/PI staining. The proportions of Annexin V+/PI- and Annexin V+/PI+ cells indicated apoptosis. The protein expression was examined by Western blot after lysing cells, and β-tublin was used as loading control. The representative charts, quantified results and Western blot results (C) of three independent experiments were shown. The statistical significance between two groups was determined with Student's t-test. **P*<0.05 and ***P*<0.01 vs. corresponding control.

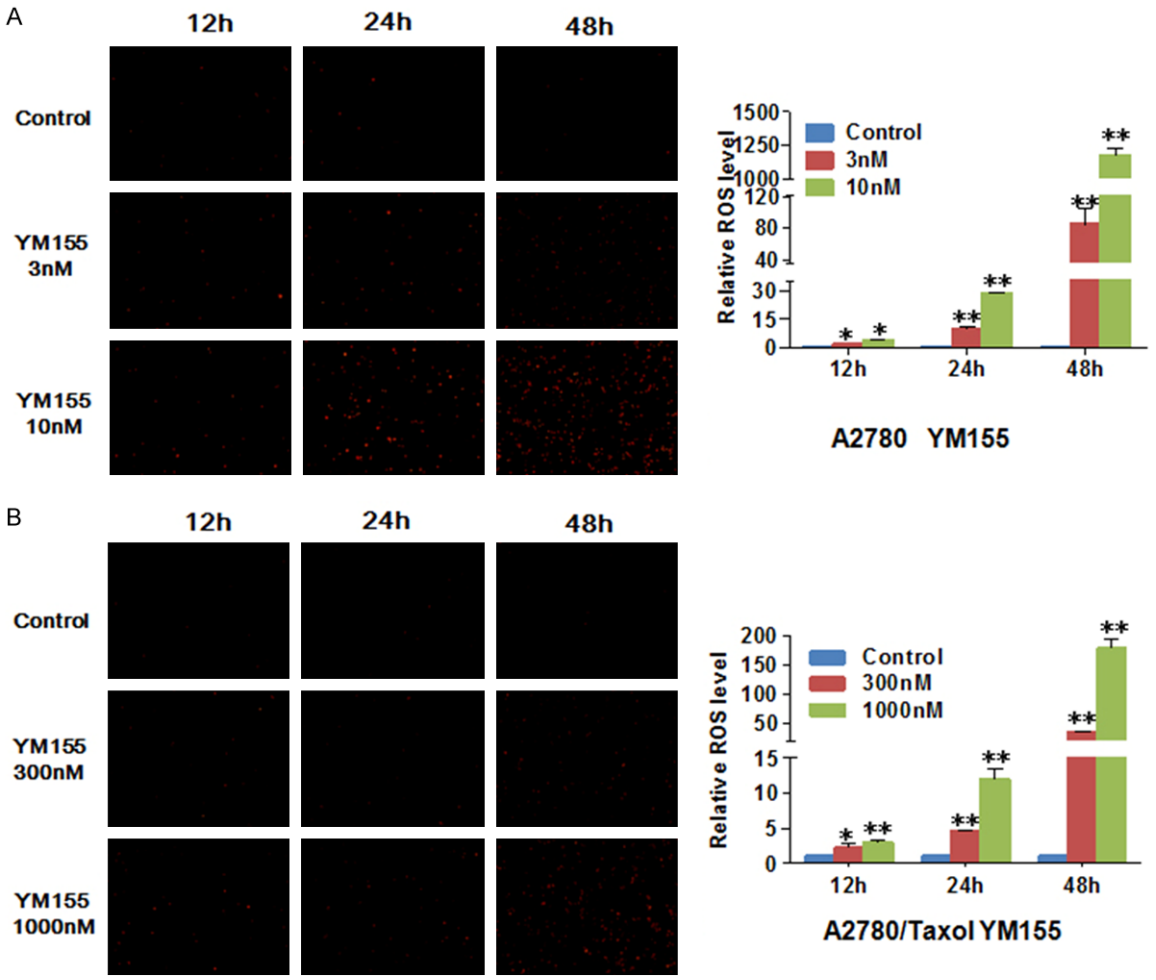

Figure 4. YM155 increases the intracellular ROS in ovarian cancer cells. A2780 (A) and A2780/Taxol (B) cells were treated with YM155 at the indicated times and concentrations, stained with DHE and photographed under florescent microscope. The representative micrographs and quantified results of three independent experiments are shown. The statistical significance between two groups was determined with Student's t-test. **P*<0.05 and ***P*<0.01 vs. corresponding control.

YM155 triggers apoptosis in ovarian cancer cells

To determine whether the growth inhibition of ovarian cancer cells by YM155 was due to apoptosis, cell apoptosis was assessed after treating A2780 and A2780/Taxol cells with YM155. As shown in **Figure 3A** and **3B**, YM155 in the dose dependent manner triggered apoptosis in both cells. To further investigate the molecular mechanism of cell apoptosis by YM155, the expression of apoptosis related proteins were detected by Western blot. YM155 in the dose dependent manner enhanced the protein levels of cleaved PARP, Bax and Mcl-1, but weakened the protein levels of pAKT S473 and pERK T202/Y204 in both cells (**Figure 3C**).

Role of ROS in the effect of YM155 on ovarian cancer cells

To examine the effect of YM155 on the intercellular ROS in ovarian cancer cells, A2780 and A2780/Taxol cells were stained with the ROS fluorescent probe DHE after YM155 treatment. As shown in **Figure 4**, YM155 dose- and time-dependently augmented the fluorescent intensity of DHE in both cells. To further explore the role of ROS in YM155-induced apoptosis in ovarian cancer cells, both A2780 and A2780/Taxol cells were treated with YM155 for 48h with or without antioxidative agents NAC and GSH pretreated for 1 h. As shown in **Figure 5A** and **5B**, NAC or GSH partially reversed YM155-induced ROS accumulation only in A2780 cells,

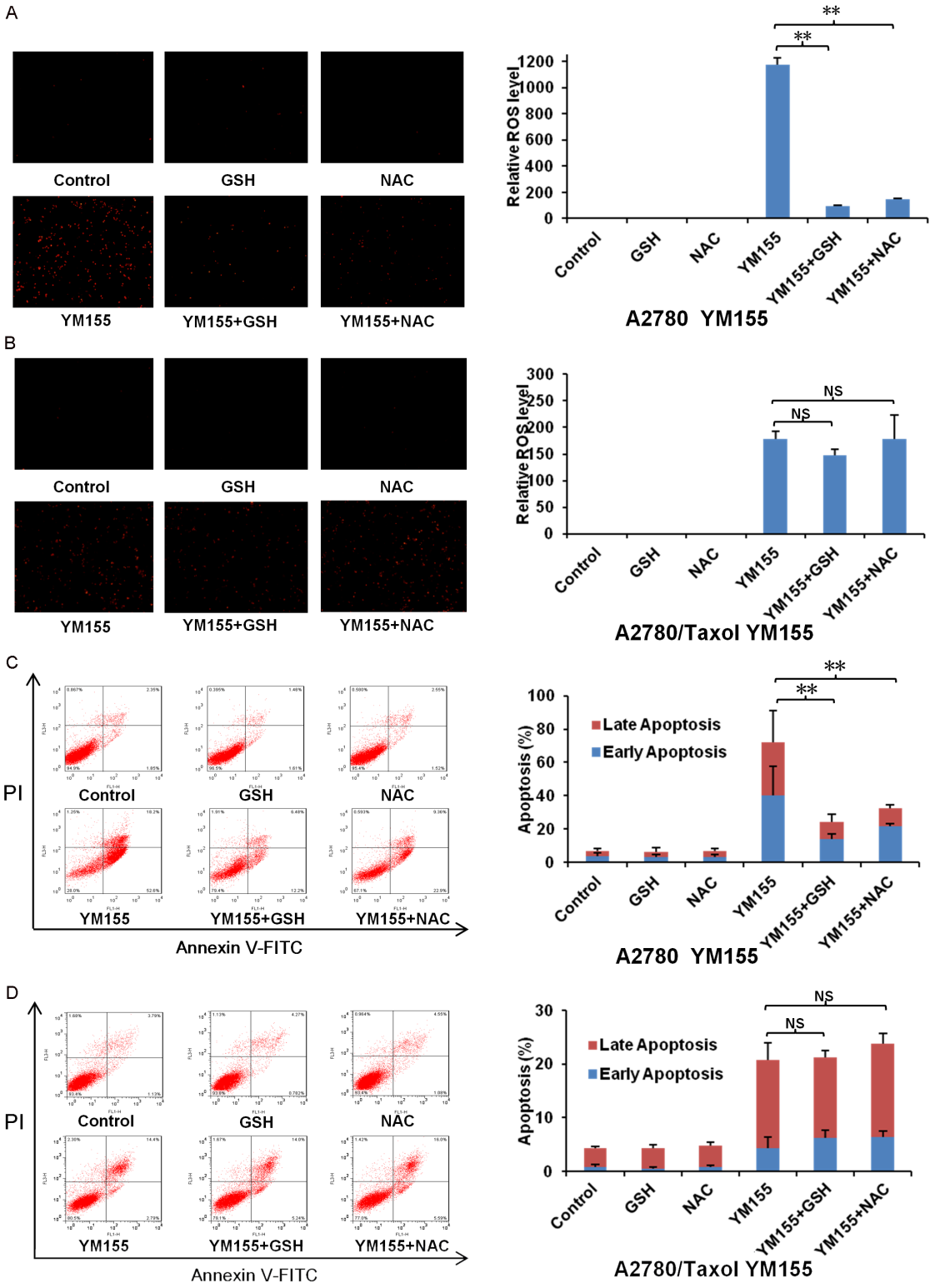

Figure 5. Effect of ROS inhibition on YM155-induced apoptosis in ovarian cancer cells. A2780 (A, C) and A2780/Taxol (B, D) cells were treated with YM155 (10 nM and 1000 nM, respectively)for 48 h with or without the NAC (10 mM) or GSH (10 mM) pretreatment for 1 h, stained with DHE and photographed under fluorescent microscope. The apoptosis was detected by FCM with Annexin V/PI staining. The proportions of Annexin V+/PI- and Annexin V+/PI+ cells indicated apoptosis. The representative micrographs, charts and quantified results of three independent experiments are shown. The statistical significance between two groups was determined with Student's t-test. NS: no significance. *P<0.05 and **P<0.01 vs. corresponding group.

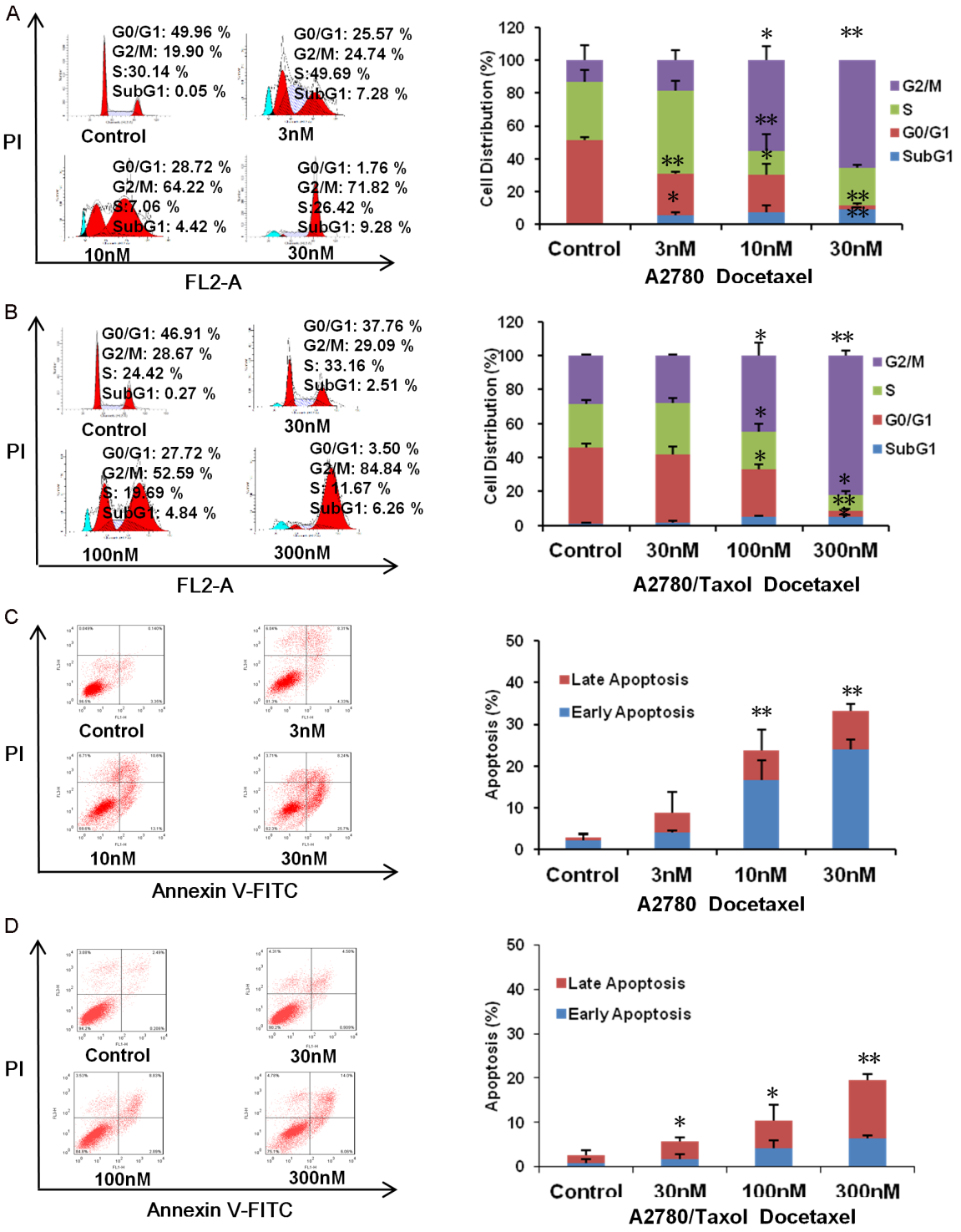

Figure 6. Docetaxel induces cell cycle arrest and apoptosis in ovarian cancer cells. A2780 (A, C) and A2780/Taxol (B, D) cells were treated with docetaxel at the indicated concentrations for 48 h. The distribution of cell cycle was detected by FCM with PI staining. The percentages of subG1, G1/G0, S, G2/M phase were calculated using ModFit LT 3.0 software. The apoptosis were detected by FCM with Annexin V/PI staining. The proportions of Annexin V+/PI- and Annexin V+/PI+ cells indicated apoptosis. The representative charts and quantified results of three independentexperiments were shown. The statistical significance between two groups was determined with Student's t-test. **P*<0.05 and ***P*<0.01 vs. corresponding control.

A

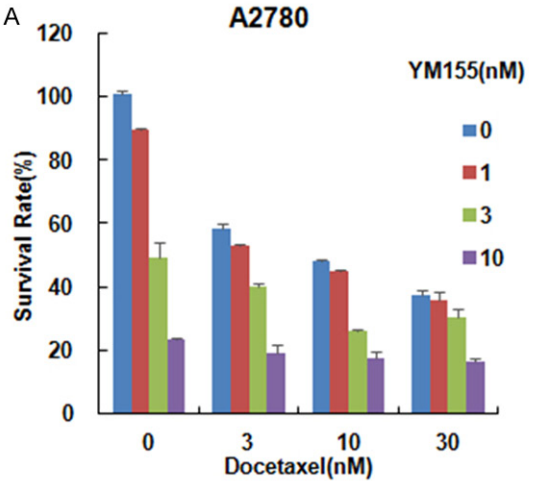

A2780

Dose YM155	Dose DTX	Effect	CI
1	3	0.5314	0.84107
1	10	0.4481	0.97444
1	30	0.359	0.99450
3	3	0.4013	0.72497
3	10	0.262	0.45810
3	30	0.3019	0.84193
10	3	0.1924	0.96215
10	10	0.1719	0.88474
10	30	0.1655	0.88805

B

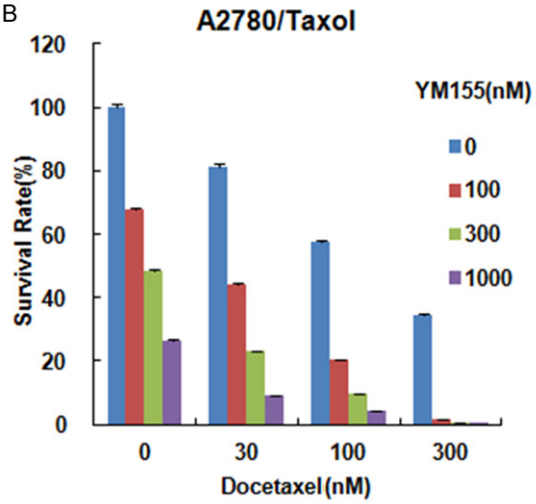

A2780/Taxol

Dose YM155	Dose DTX	Effect	CI
100	30	0.441	0.43114
100	100	0.2056	0.21873
100	300	0.0195	0.03021
300	30	0.2306	0.28487
300	100	0.099	0.1225
300	300	0.0068	0.01033
1000	30	0.0909	0.19819
1000	100	0.0442	0.08965
1000	300	0.003	0.00537

Figure 7. YM155 enhances docetaxel efficacy to inhibit the growth of ovarian cancer cells. A2780 (A) and A2780/Taxol (B) cells were treated with the indicated concentrations of YM155 and docetaxel for 72 h, and cell survival was detected by MTT assay. The data were analyzed by CompuSyn software with the results shown as growth histogram, dose-effect curve, CI values and normalized isobologram.

but not in A2780/Taxol cells. Similarly, NAC or GSH partially rescued YM155-induced apoptosis only in A2780 cells, but not in A2780/Taxol cells (**Figure 5C** and **5D**).

YM155 enhances docetaxel efficacy in ovarian cancer cells

To investigate the combined effects of YM155 and docetaxel on ovarian cancer cells, the effects of docetaxel on cell cycle and apoptosis were detected. As shown in **Figure 6A** and **6B**, docetaxel dose-dependently induced cell accumulation at subG1 and G2/M phase and reduction at S and G0/G1 phase in both A2780 and A2780/Taxol cells. Moreover, docetaxel in the dose dependent manner triggered apoptosis in both cells (**Figure 6C** and **6D**). Then cell survival was detected under the different dose combination of YM155 and docetaxel. Compared with YM155 or docetaxel alone treatment in both cells, the survival of ovarian cells was significantly decreased after combined treatment. All CI values of both cells were <1, suggesting that combination treatment was synergistic to inhibit the growth of ovarian cancer cells (**Figure 7A** and **7B**). Furthermore, the combination of YM155 and docetaxel caused more apoptosis than YM155 or docetaxel alone in both cells (**Figure 8A** and **8B**). Additionally, the protein levels of C-PARP, Bax and Mcl-1 were increased more in the co-treatment group than those in YM155 or docetaxel alone group in both cells (**Figure 8C**). Together, these results suggested

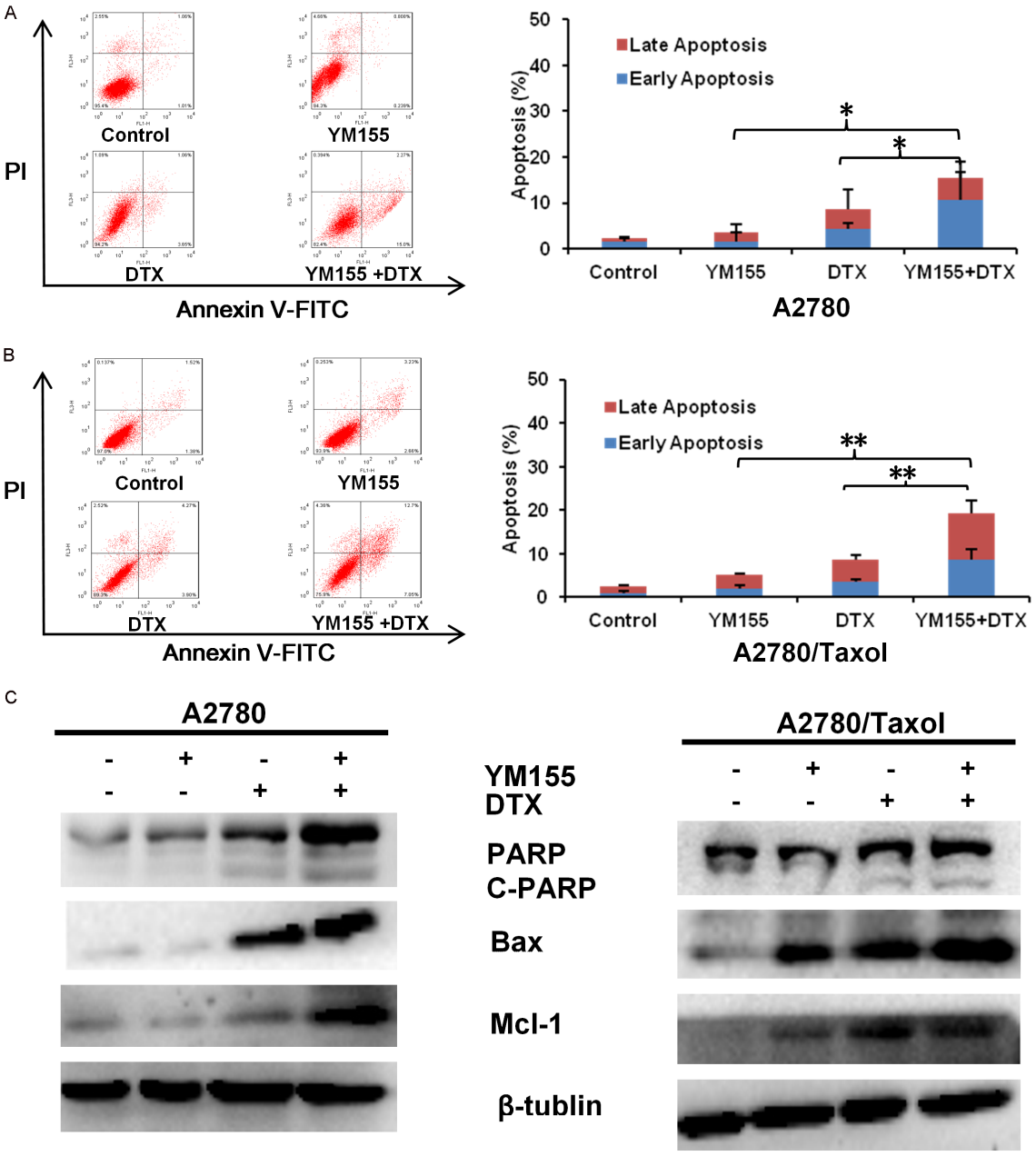

Figure 8. YM155 enhances docetaxel efficacy to induce apoptosis in ovarian cancer cells. A2780 (A) cells were treated with 1 nM YM155, 3 nM docetaxel alone or combination for 48 h. A2780/Taxol (B) cells were treated with 100 nM YM155, 100 nM docetaxel alone or combination for 48 h. The apoptosis was detected by FCM Annexin V/PI staining. The proportions of Annexin V+/PI- and Annexin V+/PI+ cells indicated the early and late stage of apoptosis. The protein expression was examined by Western blot after lysing cells, and β-tublin was used as loading control. The representative charts, quantified results and Western blot results (C) of three independent experiments were shown. The statistical significance between two groups was determined with Student's t-test. DTX: Docetaxel. **P*<0.05 and ***P*<0.01 vs. corresponding control.

that YM155 was able to enhance docetaxel efficacy in ovarian cancer cells.

Discussion

In the current study, our data presented that the ABCB1-overexpressing taxol resistant ovarian cancer cells A2780/Taxol showed about 87 folds resistance to both YM155 and docetaxel compared with the parental A2780 cells. This phenomenon is probably explained by previous studies which have demonstrated that YM155 is a substrate of ABCB1, and overexpressing of ABCB1 can cause YM155 efflux to mediated

YM155-specific resistance [31, 32]. YM155 significantly induced cell cycle arrest and apoptosis with the increasing intracellular ROS levels in ovarian cancer cells. Suppression of ROS generation partially rescued YM155-induced apoptosis only in the parental A2780 cells, but not in the resistant A2780/Taxol cells, suggesting that ROS might play the diverse roles in YM155-induced apoptosis in the different ovarian cancer cells.

It is valuable to overcome docetaxel resistance or enhance docetaxel sensitivity for the treatment of cancers. Our results showed that YM155 enhanced docetaxel efficacy to inhibit the growth and induce apoptosis in either parental or resistant ovarian cancer cells. Similarly with our data, YM155 has been reported synergistically to enhance the efficacies of microtubule-targeting agents, including paclitaxel, docetaxel and vinorelbine in triple-negative breast cancer cells [33]. YM155 in combination with docetaxel induced more apoptosis and showed greater efficacy than either agent alone in human malignant melanoma models [34]. YM155 also promoted docetaxel-induced apoptosis and tumor regression in human lung cancer xenograft models [35]. Although these preclinical data are encouraging, the clinical results of YM155 and docetaxel combination for the treatment of cancers are not optimistic. A phase II, multicenter, open-label study of YM155 plus docetaxel in patients with stage III (unresectable) or stage IV melanoma has shown that YM155 was generally well tolerated with modest activity when plus docetaxel, but the predetermined primary efficacy endpoint was not achieved [36]. Another phase II, multicenter, open-label, randomized study of YM155 plus docetaxel as first-line treatment in patients with HER2-negative metastatic breast cancer has exhibited that there was no statistically significant differences in the endpoints between combination and docetaxel alone [37]. In a phase I/II study of YM155 combined with paclitaxel and carboplatin in patients with advanced non-small-cell lung cancer, this combination exhibited a favorable safety profile but failed to demonstrate an improvement in response rates [38]. Therefore, whether the combination of YM155 and docetaxel improves clinical outcomes in ovarian cancer patients remains to be determined.

In summary, our study provides the evidence that YM155 can enhance docetaxel efficacy in ovarian cancer cells. Combination of YM155 and docetaxel may be a feasible strategy for the treatment of ovarian cancer.

Acknowledgements

This work was supported by funds from the National Natural Science Foundation of China No. 81661148049, No. 81772540 (Z. S.), No. 81503293 (X. J. Y.) and No. 81373075 (R. Y. O), the Guangdong Natural Science Funds for Distinguished Young Scholar No. 2014A030306001 (Z. S.), the Guangdong Special Support Program for Young Talent No. 2015TQ01R350 (Z. S.), the Science and Technology Program of Guangdong No. 2016A050502027 (Z. S.) and the Science and Technology Program of Guangzhou No. 201704030058 (Z. S.).

Disclosure of conflict of interest

None.

Address correspondence to: Dr. Zhi Shi, Department of Cell Biology & Institute of Biomedicine, National Engineering Research Center of Genetic Medicine, Guangdong Provincial Key Laboratory of Bioengineering Medicine, College of Life Science and Technology, Jinan University, Room 708, The 2nd Engineer and Scientific Building, 601 Huangpu Road West, Guangzhou 510632, Guangdong, China. Tel: +86-20-852-245-25; Fax: +86-20-852-259-77; E-mail: tshizhi@jnu.edu.cn; Dr. Xiao-Jian Yan, Department of Gynecology, The First Affiliated Hospital of Wenzhou Medical University, Shangcai Village South, Ouhai District, Wenzhou 325000, Zhejiang, China. Tel: +86- 577-555-791-63; Fax: +86-577-555-780-33; E-mail: yxjbetter@126.com

References

[1] Wang S, Qiu J, Shi Z, Wang Y and Chen M. Nanoscale drug delivery for taxanes based on the mechanism of multidrug resistance of cancer. Biotechnol Adv 2015; 33: 224-241.

[2] Zheng WE, Chen H, Yuan SF, Wu LL, Zhang W, Sun HY and Chen WJ. Overexpression of beta-III-tubulin and survivin associated with drug resistance to docetaxel-based chemotherapy in advanced gastric cancer. J BUON 2012; 17: 284-290.

[3] Yuan SF, Zhu LJ, Zheng WE, Chen H, Wu LL, Zhang W, Sun HY and Chen WJ. Expression of beta-tubulin III and survivin in advance stage breast cancer correlates with chemotherapeutic effects of docetaxel. Asian Pac J Cancer Prev 2012; 13: 361-365.

[4] Wang XW, Wang XK, Zhang X, Liang YJ, Shi Z, Chen LM and Fu LW. FG020326 sensitized multidrug resistant cancer cells to docetaxel-mediated apoptosis via enhancement of caspases activation. Molecules 2012; 17: 5442-5458.
[5] Hopper-Borge E, Chen ZS, Shchaveleva I, Belinsky MG and Kruh GD. Analysis of the drug resistance profile of multidrug resistance protein 7 (ABCC10): resistance to docetaxel. Cancer Res 2004; 64: 4927-4930.
[6] De Iuliis F, Salerno G, Giuffrida A, Milana B, Taglieri L, Rubinacci G, Giantulli S, Terella F, Silvestri I and Scarpa S. Breast cancer cells respond differently to docetaxel depending on their phenotype and on survivin upregulation. Tumour Biol 2016; 37: 2603-2611.
[7] Meng H, Tanigawa N, Hao CY, Dai DJ, Lu CD and Ji JF. Chemoresponse to docetaxel correlates with expression of the survivin splicing variants in patients with gastric cancer. Hepatogastroenterology 2007; 54: 1934-1940.
[8] Altieri DC. Survivin, cancer networks and pathway-directed drug discovery. Nat Rev Cancer 2008; 8: 61-70.
[9] Yamauchi T, Nakamura N, Hiramoto M, Yuri M, Yokota H, Naitou M, Takeuchi M, Yamanaka K, Kita A, Nakahara T, Kinoyama I, Matsuhisa A, Kaneko N, Koutoku H, Sasamata M, Kobori M, Katou M, Tawara S, Kawabata S and Furuichi K. Sepantronium bromide (YM155) induces disruption of the ILF3/p54(nrb) complex, which is required for survivin expression. Biochem Biophys Res Commun 2012; 425: 711-716.
[10] Nakamura N, Yamauchi T, Hiramoto M, Yuri M, Naito M, Takeuchi M, Yamanaka K, Kita A, Nakahara T, Kinoyama I, Matsuhisa A, Kaneko N, Koutoku H, Sasamata M, Yokota H, Kawabata S and Furuichi K. Interleukin enhancer-binding factor 3/NF110 is a target of YM155, a suppressant of survivin. Mol Cell Proteomics 2012; 11: M111 013243.
[11] Tao YF, Lu J, Du XJ, Sun LC, Zhao X, Peng L, Cao L, Xiao PF, Pang L, Wu D, Wang N, Feng X, Li YH, Ni J, Wang J and Pan J. Survivin selective inhibitor YM155 induce apoptosis in SK-NEP-1 Wilms tumor cells. BMC Cancer 2012; 12: 619.
[12] Nakahara T, Kita A, Yamanaka K, Mori M, Amino N, Takeuchi M, Tominaga F, Hatakeyama S, Kinoyama I, Matsuhisa A, Kudoh M and Sasamata M. YM155, a novel small-molecule survivin suppressant, induces regression of established human hormone-refractory prostate tumor xenografts. Cancer Res 2007; 67: 8014-8021.
[13] Kita A, Nakahara T, Yamanaka K, Nakano K, Nakata M, Mori M, Kaneko N, Koutoku H, Izumisawa N and Sasamata M. Antitumor effects of YM155, a novel survivin suppressant, against human aggressive non-Hodgkin lymphoma. Leuk Res 2011; 35: 787-792.
[14] Yamanaka K, Nakata M, Kaneko N, Fushiki H, Kita A, Nakahara T, Koutoku H and Sasamata M. YM155, a selective survivin suppressant, inhibits tumor spread and prolongs survival in a spontaneous metastatic model of human triple negative breast cancer. Int J Oncol 2011; 39: 569-575.
[15] Rauch A, Hennig D, Schafer C, Wirth M, Marx C, Heinzel T, Schneider G and Kramer OH. Survivin and YM155: how faithful is the liaison? Biochim Biophys Acta 2014; 1845: 202-220.
[16] Nakahara T, Kita A, Yamanaka K, Mori M, Amino N, Takeuchi M, Tominaga F, Kinoyama I, Matsuhisa A, Kudou M and Sasamata M. Broad spectrum and potent antitumor activities of YM155, a novel small-molecule survivin suppressant, in a wide variety of human cancer cell lines and xenograft models. Cancer Sci 2011; 102: 614-621.
[17] Mir R, Stanzani E, Martinez-Soler F, Villanueva A, Vidal A, Condom E, Ponce J, Gil J, Tortosa A and Gimenez-Bonafe P. YM155 sensitizes ovarian cancer cells to cisplatin inducing apoptosis and tumor regression. Gynecol Oncol 2014; 132: 211-220.
[18] Shi Z, Liang YJ, Chen ZS, Wang XW, Wang XH, Ding Y, Chen LM, Yang XP and Fu LW. Reversal of MDR1/P-glycoprotein-mediated multidrug resistance by vector-based RNA interference in vitro and in vivo. Cancer Biol Ther 2006; 5: 39-47.
[19] Weil CS. Tables for convenient calculation of median-effective dose (LD50 or ED50) and instructions in their use. Biometrics 1952; 8: 249-263.
[20] Chou TC, Talalay P. Quantitative analysis of dose-effect relationships: the combined effects of multiple drugs or enzyme inhibitors. Adv Enzyme Regul 1984; 22: 27-55.
[21] Jiang QW, Cheng KJ, Mei XL, Qiu JG, Zhang WJ, Xue YQ, Qin WM, Yang Y, Zheng DW, Chen Y, Wei MN, Zhang X, Lv M, Chen MW, Wei X and Shi Z. Synergistic anticancer effects of triptolide and celastrol, two main compounds from thunder god vine. Oncotarget 2015; 6: 32790-32804.
[22] Chen X, Gong L, Ou R, Zheng Z, Chen J, Xie F, Huang X, Qiu J, Zhang W, Jiang Q, Yang Y, Zhu H, Shi Z and Yan X. Sequential combination therapy of ovarian cancer with cisplatin and gamma-secretase inhibitor MK-0752. Gynecol Oncol 2016; 140: 537-544.
[23] Lv M, Qiu JG, Zhang WJ, Jiang QW, Qin WM, Yang Y, Zheng DW, Chen Y, Huang JR, Wang K, Wei MN, Cheng KJ and Shi Z. Wallichinine re-

verses ABCB1-mediated cancer multidrug resistance. Am J Transl Res 2016; 8: 2969-2980.
[24] Shi Z, Park HR, Du Y, Li Z, Cheng K, Sun SY, Fu H and Khuri FR. Cables1 complex couples survival signaling to the cell death machinery. Cancer Res 2015; 75: 147-158.
[25] Shi Z, Li Z, Li ZJ, Cheng K, Du Y, Fu H and Khuri FR. Cables1 controls p21/Cip1 protein stability by antagonizing proteasome subunit alpha type 3. Oncogene 2015; 34: 2538-2545.
[26] Xie FF, Pan SS, Ou RY, Zheng ZZ, Huang XX, Jian MT, Qiu JG, Zhang WJ, Jiang QW, Yang Y, Li WF, Shi Z and Yan XJ. Volasertib suppresses tumor growth and potentiates the activity of cisplatin in cervical cancer. Am J Cancer Res 2015; 5: 3548-3559.
[27] Gong LH, Chen XX, Wang H, Jiang QW, Pan SS, Qiu JG, Mei XL, Xue YQ, Qin WM, Zheng FY, Shi Z and Yan XJ. Piperlongumine induces apoptosis and synergizes with cisplatin or paclitaxel in human ovarian cancer cells. Oxid Med Cell Longev 2014; 2014: 906804.
[28] Zheng DW, Xue YQ, Li Y, Di JM, Qiu JG, Zhang WJ, Jiang QW, Yang Y, Chen Y, Wei MN, Huang JR, Wang K, Wei X and Shi Z. Volasertib suppresses the growth of human hepatocellular carcinoma in vitro and in vivo. Am J Cancer Res 2016; 6: 2476-2488.
[29] Yang Y, Qiu JG, Li Y, Di JM, Zhang WJ, Jiang QW, Zheng DW, Chen Y, Wei MN, Huang JR, Wang K and Shi Z. Targeting ABCB1-mediated tumor multidrug resistance by CRISPR/Cas9-based genome editing. Am J Transl Res 2016; 8: 3986-3994.
[30] Xu H, Hong FZ, Li S, Zhang P and Zhu L. Short hairpin RNA-mediated MDR1 gene silencing increases apoptosis of human ovarian cancer cell line A2780/Taxol. Chin J Cancer Res 2012; 24: 138-142.
[31] Iwai M, Minematsu T, Li Q, Iwatsubo T and Usui T. Utility of P-glycoprotein and organic cation transporter 1 double-transfected LLC-PK1 cells for studying the interaction of YM155 monobromide, novel small-molecule survivin suppressant, with P-glycoprotein. Drug Metab Dispos 2011; 39: 2314-2320.
[32] Voges Y, Michaelis M, Rothweiler F, Schaller T, Schneider C, Politt K, Mernberger M, Nist A, Stiewe T, Wass MN, Rodel F and Cinatl J. Effects of YM155 on survivin levels and viability in neuroblastoma cells with acquired drug resistance. Cell Death Dis 2016; 7: e2410.
[33] Kaneko N, Yamanaka K, Kita A, Tabata K, Akabane T and Mori M. Synergistic antitumor activities of sepantronium bromide (YM155), a survivin suppressant, in combination with microtubule-targeting agents in triple-negative breast cancer cells. Biol Pharm Bull 2013; 36: 1921-1927.
[34] Yamanaka K, Nakahara T, Yamauchi T, Kita A, Takeuchi M, Kiyonaga F, Kaneko N and Sasamata M. Antitumor activity of YM155, a selective small-molecule survivin suppressant, alone and in combination with docetaxel in human malignant melanoma models. Clin Cancer Res 2011; 17: 5423-5431.
[35] Nakahara T, Yamanaka K, Hatakeyama S, Kita A, Takeuchi M, Kinoyama I, Matsuhisa A, Nakano K, Shishido T, Koutoku H and Sasamata M. YM155, a novel survivin suppressant, enhances taxane-induced apoptosis and tumor regression in a human Calu 6 lung cancer xenograft model. Anticancer Drugs 2011; 22: 454-462.
[36] Kudchadkar R, Ernst S, Chmielowski B, Redman BG, Steinberg J, Keating A, Jie F, Chen C, Gonzalez R and Weber J. A phase 2, multicenter, open-label study of sepantronium bromide (YM155) plus docetaxel in patients with stage III (unresectable) or stage IV melanoma. Cancer Med 2015; 4: 643-650.
[37] Clemens MR, Gladkov OA, Gartner E, Vladimirov V, Crown J, Steinberg J, Jie F and Keating A. Phase II, multicenter, open-label, randomized study of YM155 plus docetaxel as first-line treatment in patients with HER2-negative metastatic breast cancer. Breast Cancer Res Treat 2015; 149: 171-179.
[38] Kelly RJ, Thomas A, Rajan A, Chun G, Lopez-Chavez A, Szabo E, Spencer S, Carter CA, Guha U, Khozin S, Poondru S, Van Sant C, Keating A, Steinberg SM, Figg W and Giaccone G. A phase I/II study of sepantronium bromide (YM155, survivin suppressor) with paclitaxel and carboplatin in patients with advanced non-small-cell lung cancer. Ann Oncol 2013; 24: 2601-2606.